Determination of Steady-State Elongational Viscosity for Rubber Compounds Using Bell-Mouthed Dies

J. CLARKE,[1] J. PETERA[2]

[1] Rubber Process Engineering Centre, Institute of Polymer Technology and Materials Engineering, Loughborough University, Loughborough, Leicestershire LE11 3TU, United Kingdom

[2] Department of Process and Environmental Engineering, Lodz Technical University, ul. Wólczańska Nr 175, 90-924 Lodz, Poland

Received 31 July 1996; accepted 5 February 1997

ABSTRACT: A bell-mouthed die geometry was designed to cause convergent flow at a constant, uniform, elongational strain rate. An equation was derived, which showed that steady-state elongational viscosity could be calculated from a plot of pressure drop due to elongation against a simple function of die length. To obtain values of pressure drop due to elongation, it was necessary to correct the total pressure drop measured across the bell-mouthed dies for the contribution from shear occurring near the die wall. For this purpose, a simplified shape for the bell-mouthed dies was assumed, comprising several parallel sided segments. Applying a formula to pressure drop data measured across straight dies corresponding to these segments gave an estimate of the pressure drop due to shear across the bell-mouthed dies. Pressure drops due to elongation were determined by subtracting the pressure drop due to shear from the total pressure drop measured across the bell-mouthed dies. Measurements were also carried out with lubrication to validate the shear correction method. The results indicate that for the compound used in this study, a combination of bell-mouthed and straight-sided dies can be used in a conventional capillary rheometer to determine steady-state elongational viscosity. An elongational viscosity of 190 kPa s at 90°C and at a strain rate of 10 s^{-1} was determined for a simple styrene–butadiene rubber compound.
 J Appl Polym Sci **66:** 1139–1150, 1997

Key words: elongational viscosity; rubber; convergent flow; capillary rheometer

INTRODUCTION

Practically all rubber processing operations involve a substantial amount of convergent flow, which results in elongational deformation. The most obvious case is extrusion, where material passes from a large cross section in the barrel to a small cross section in the die. Elongational deformation during extrusion is not only important in determining the level of back pressure, but also affects the extent of die swell resulting from elongational relaxation.[1] Somewhat less obviously, convergent flow occurs during mixing, where material in front of the rotor wing is forced through the small clearance between the chamber wall and the tip of the wing. The significance of elongational flow during mixing is that the stresses reached are higher than in shear flow; hence, the rates of filler dispersion tend to be greater.[2–4]

Despite the obvious importance of elongational rheology, it is the shear behavior of rubbers that receives the most attention, mostly because of the ease of measurement. By contrast, elongational rheology is very difficult to assess, and there is no well-established, simple way of measuring steady-

Correspondence to: J. Clarke.

Journal of Applied Polymer Science, Vol. 66, 1139–1150 (1997)
 CCC 0021-8995/97/061139-12

state elongational viscosity at the relatively high strain rates likely to be encountered during processing. With the advent of finite element analysis (FEA) techniques capable of modelling complicated geometries and potentially complex material behavior, it has become particularly important to be able to accurately quantify all aspects of flow behavior, including elongational viscosity.

Attempts to develop methods of quantifying elongational rheology at relatively high strain rates have generally centered around spinning experiments[5–9] and the analysis of convergent flow regimes.[1,10–12] For applicability to rubber processing and the ability to achieve a steady rate of deformation, the use of convergent flows to determine elongational viscosity is clearly more suitable. Cogswell published a review of convergent flow analysis and suggested an ideal converging flow rheometer for measuring elongational rheology.[1] One of the main problems encountered in using convergent flow is the occurrence of shear at the die wall, which makes analysis more difficult. Lubrication has been used to overcome this problem, although the thickness of the lubricating layer complicates die design, and the requirement for ancillary equipment makes experimentation more difficult.[13,14] James et al. did not use lubrication but made allowance for shear theoretically; however, because of assumptions made, this correction is rather unsatisfactory.[12] A further problem with their method is the technical difficulty of measurement and the need for custom-made pressure transducers.

Our approach is similar to that of James et al.,[12] but the equipment is simpler, and the correction for shear is more practical. The basic apparatus used is an ordinary capillary rheometer fitted with a single pressure transducer in the barrel. The use of bell-mouthed dies of different lengths negates the use of several pressure transducers. Allowance for shear is made by practical measurements using parallel sided dies of varying diameters and lengths. This experimental method is a more satisfactory means of shear correction than a purely theoretical one and also means that it is not necessary to use lubrication, with its attendant technical and theoretical difficulties.

THEORY

Converging Die Geometry

In order to determine elongational viscosity experimentally, a steady rate of extension should ideally be reached during measurement. We can say that a material is subjected to homogeneous steady simple extension in a flow that is spatially uniform with a constant rate of elongation $\dot{\varepsilon}$ in the x_1-direction and $-\frac{1}{2}\dot{\varepsilon}$ in any direction perpendicular to the x_1-direction.[2] The ratio of net tensile stress ($\sigma_E = \sigma_{11} - \sigma_{22}$) to rate of strain is monitored as a function of time and elongational viscosity (η_E) is defined as

$$\eta_E = \lim_{t\to\infty} \frac{\sigma_E}{\dot{\varepsilon}}$$

However, this definition is very difficult to realize in practice, even with highly viscous liquids; and great care is needed, for example, in satisfying uniformity of flow, for reliable measurements to be obtained.[10,15]

It is well known that for fluid flow in a converging geometry, a substantial contribution to the resultant pressure drop has its origin in elongational deformation. Thus, in principle, the geometry can be used for measuring elongational viscosity, provided that the elongation rate is constant over the whole domain, or at least a predominant part of the domain. In addition to achieving steady elongation in this way, the shear contribution should be eliminated or reduced to a minimum. The derivation below leads to a definition of a converging geometry, which assures a constant elongation rate.

To conserve continuity, the volumetric flow rate (V) along a die must be constant and thus, the mean velocity (v) increases rapidly as the radius of the die (R) decreases along the axial direction (z), according to

$$v = \frac{V}{\pi R^2} \tag{1}$$

From the definition of rate of elongation,[16] after differentiating eq. (1),

$$\frac{\partial v_z}{\partial z} = \dot{\varepsilon} = -\frac{V}{\pi}\frac{2}{R^2}\frac{dR}{dz} \tag{2}$$

and integration by separation of the variables,

$$\int_{R_o}^{r(z)} \frac{dR}{R^3} = -\frac{\pi\dot{\varepsilon}}{2V}\int_0^z dz \tag{3}$$

one obtains

$$\frac{1}{r(z)^2} - \frac{1}{R_0^2} = \frac{\pi\dot{\varepsilon}}{V} z \tag{4}$$

where R_0 is the maximum radius of the die at the inlet. After rearranging, one obtains an equation describing the converging geometry as a function of axial position.

$$r(z) = \frac{R_0}{\sqrt{1 + \frac{\dot{\varepsilon}}{v_0} z}} \tag{5}$$

Equation (5) can be reformulated as follows:

$$r(z) = \frac{R_0}{\sqrt{1 + Az}}, \quad A = \frac{\dot{\varepsilon}}{v_0} \tag{6}$$

indicating that A is a geometric constant determining the rate of convergence and which is related to the elongational rate and the mean inlet velocity $v_0 = V/\pi R_0^2$.

The Main Assumptions

The rheological behavior of rubber must be taken into consideration when analyzing convergent flow with a view to obtaining elongational viscosity. For small deformations, rubber behaves as an elastic solid with full recovery after releasing the stress. At low rates of deformation, rubber exhibits highly viscoelastic properties with a yield stress and elastic recovery with a large spectrum of relaxation times, giving strong history-of-deformation dependence. For higher deformation rates, the non-Newtonian properties are enhanced exhibiting, for example, considerable shear thinning. As a result of the small non-Newtonian index (n), the velocity profile for flow in a parallel sided pipe is much flatter than the parabolic one observed for Newtonian liquids. Wall slippage is also very likely to occur under conditions of high stress and deformation rate.

On the basis of the above considerations and experimental observations, the main assumptions concerning flow in a converging die are illustrated in Figure 1 and can be summarized as follows: (1) Elongational deformation predominates in the core; and (2) shearing dominates flow in the vicinity of the die wall, with a high liklihood of wall slippage occurring, particularly near the die exit.

For each of the two main regions, namely, elongation in the core and the shear dominance near the wall, the following analysis using conservation of momentum is carried out in different, appropriate coordinate systems, both resulting from the converging nature of the geometry. The two coordinate systems are illustrated in Figure 2.

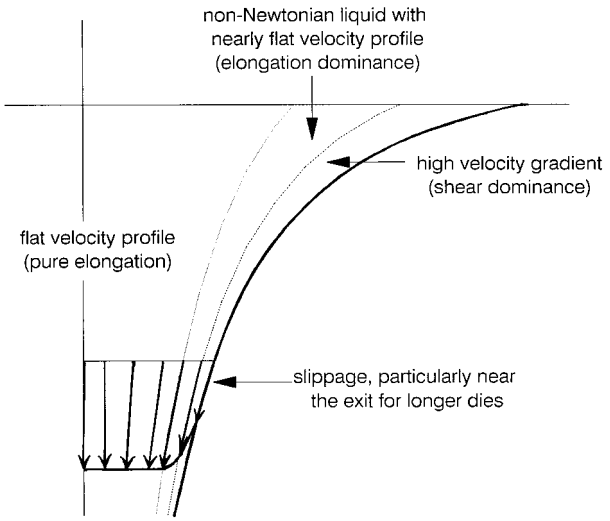

Figure 1 Diagram to show the main features and assumptions concerning flow of rubber through the bell-mouthed die.

Pure Elongation

The first coordinate system shown in Figure 2(a) is defined by the following equations, where (x, y, z) are the Cartesian coordinates and the triple (R, θ, Z) denotes the new coordinate system, intrinsic to the die geometry.

$$\begin{aligned} x &= \frac{R}{\sqrt{1 + AZ}} \cos\theta \\ y &= \frac{R}{\sqrt{1 + AZ}} \sin\theta \\ z &= Z \end{aligned} \tag{7}$$

The vectors tangent to the parametric coordinate lines (versors) are calculated as follows:

$$e_{(R)} = \begin{bmatrix} \frac{\cos\theta}{(1 + AZ)^{1/2}} \\ \frac{\sin\theta}{(1 + AZ)^{1/2}} \\ 0 \end{bmatrix} \quad e_{(\theta)} = \begin{bmatrix} \frac{-\sin\theta}{(1 + AZ)^{1/2}} \\ \frac{\cos\theta}{(1 + AZ)^{1/2}} \\ 0 \end{bmatrix}$$

$$e_{(Z)} = \begin{bmatrix} \frac{-RA\cos\theta}{(1 + AZ)^{3/2}} \\ \frac{-RA\sin\theta}{(1 + AZ)^{3/2}} \\ 1 \end{bmatrix} \tag{8}$$

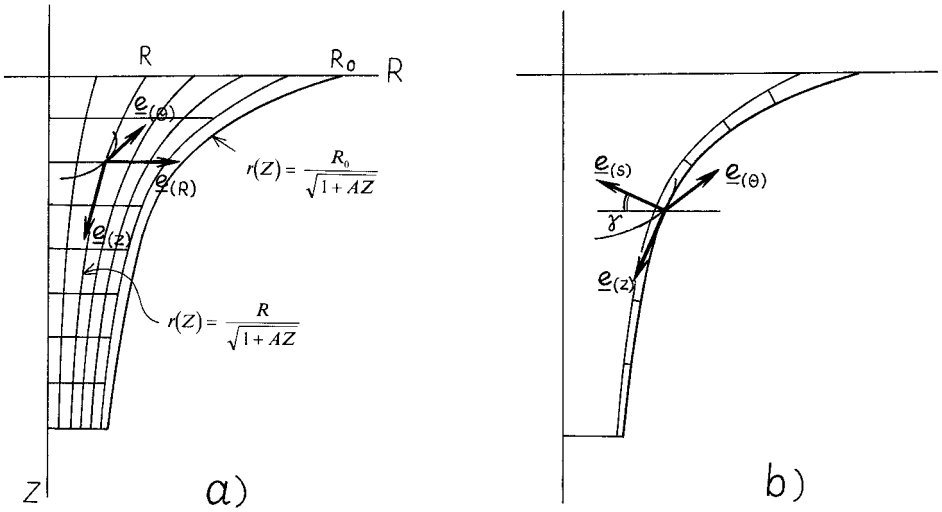

Figure 2 Two coordinate systems intrinsic to the converging geometry of the bell-mouthed die corresponding to the two main flow regimes: (a) pure elongation in the core; (b) shear dominating region near the die's wall.

The metric tensor defined as $g_{ij} = e_{(i)} \cdot e_{(j)}$ is given

$$\underline{\underline{g}} = \begin{bmatrix} \dfrac{1}{1+AZ} & 0 & \dfrac{-RA}{2(1+AZ)^2} \\ 0 & \dfrac{R^2}{1+AZ} & 0 \\ \dfrac{-RA}{2(1+AZ)^2} & 0 & 1+\dfrac{R^2A^2}{4(1+AZ)^3} \end{bmatrix} \tag{9}$$

with the determinant

$$g = \det[\underline{\underline{g}}] = \left(\frac{R}{1+AZ}\right)^2 \tag{10}$$

The momentum balance in the coordinate system defined above is formulated in terms of total stress tensor components, neglecting inertia, as follows[17]:

$$T^{ij}_{,j} = \frac{1}{g^{1/2}} \frac{\partial}{\partial x^j} (g^{1/2} T^{ij}) + T^{jk} \begin{Bmatrix} i \\ j \quad k \end{Bmatrix} = 0 \tag{11}$$

where the relationship between the contravariant and the physical stress tensor components can be established in order to obtain practically useful relationships, as follows:

$$T^{ij} = \left(\frac{g_{mm}}{g_{jj}}\right)^{1/2} g^{im} T(mj)$$

where

$$g^{im} g_{mj} = \delta^i_j \tag{12}$$

One can observe that for the axial momentum component,

$$\begin{Bmatrix} 3 \\ j \quad k \end{Bmatrix} = 0, \quad g^{Z\theta} = 0, \quad g^{ZZ} = 1$$

And after taking into account that nothing changes in the circumferential direction $\partial/\partial\theta = 0$, one can write down the momentum balance in the axial direction, as follows:

$$\frac{\partial}{\partial R}\left\{ g^{1/2}\left[g^{ZR} T(RR) + \left(\frac{g_{ZZ}}{g_{RR}}\right)^{1/2} T(ZR) \right]\right\}$$

$$+ \frac{\partial}{\partial Z}\left\{ g^{1/2}\left[\left(\frac{g_{RR}}{g_{ZZ}}\right)^{1/2} g^{ZR} T(RZ) + T(ZZ) \right]\right\} = 0 \tag{13}$$

On the basis of the first main assumption, the tangential stresses can be neglected in the core. Using the following formulae based on eqs. (9) and (10),

$$\frac{\partial}{\partial R}(g^{1/2}g^{ZR}) = \frac{RA}{(1+AZ)^2},$$

$$\frac{\partial}{\partial Z}(g^{1/2}) = -\frac{RA}{(1+AZ)^2} \quad (14)$$

one obtains the final form of the differential momentum balance equation

$$\frac{\partial T(ZZ)}{\partial Z} = \frac{A}{1+AZ}(T(ZZ) - T(RR)) \quad (15)$$

This can be integrated along the die axis. The normal stress difference in eq. (15) is responsible for pure elongation. Due to the special geometry of the bell-mouthed die, the elongation rate is constant. Thus, according to the general objectivity requirement for any rheological constitutive equation, the normal stress difference determined entirely by the elongation rate must be constant over the whole die domain or at least over the predominant core part. Noting that the total normal axial stresses at the inlet and the outlet are equal to measured pressures, one obtains the desired relationship between the pressure drop in the die on the one hand and the normal stress difference on the other

$$T(ZZ)_2 - T(ZZ)_1 = -p_2 - (-p_1) = \Delta p$$
$$= [T(ZZ) - T(RR)]\ln(1+AZ) \quad (16)$$

The elongational viscosity is defined as the ratio of the normal stress difference to the rate of elongation

$$\eta_e = \frac{T(ZZ) - T(RR)}{\dot{\varepsilon}} \quad (17)$$

Equation (16) can therefore be expressed as follows:

$$\Delta p = \eta_e \dot{\varepsilon} \ln(1 + AL) \quad (18)$$

where L is the length of a bell-mouthed die having the correct geometry. According to eq. (18), measured pressure drops due to elongation plotted against values of $\ln(1 + AL)$ for dies of different lengths should give a straight line of slope $\eta_e\dot{\varepsilon}$. Dividing this value by the elongational strain rate would then give the elongational viscosity (η_e).

The Shear Correction Formula

According to the second main assumption, that shearing dominates flow in the vicinity of the die wall, the analysis of shear flow should be carried out in a thin layer adjacent to the die wall. A good approximation for the geometry of this thin layer is provided by a coordinate system determined strictly by the wall geometry, as shown in Figure 2(b). The versors are defined again, this time in an orthogonal system. It should be emphasized that the S-coordinate (as well as its versor) is orthogonal to the die wall and remains the same across the shear layer.

The versors are

$$e_{(s)} = \begin{bmatrix} \cos\gamma\cos\theta \\ \cos\gamma\sin\theta \\ \sin\gamma \end{bmatrix} \quad e_{(\theta)} = \begin{bmatrix} -r_0\sin\theta \\ r_0\cos\theta \\ 0 \end{bmatrix}$$

$$e_{(Z)} = \begin{bmatrix} -\dfrac{r_0 A\cos\theta}{1+AZ} \\ -\dfrac{r_0 A\sin\theta}{1+AZ} \\ 1 \end{bmatrix} \quad (19)$$

where

$$r_0 = \frac{R_0}{\sqrt{1+AZ}}, \quad \cos\gamma = \frac{1}{\sqrt{1+\dfrac{R_0 A}{4(1+AZ)^3}}},$$

$$\sin\gamma = \frac{R_0 A}{2(1+AZ)^{3/2}}\cos\gamma \quad (20)$$

They define the diagonal metric tensor

$$\underline{\underline{g}} = \begin{bmatrix} 1 & 0 & 0 \\ 0 & \dfrac{R_0^2}{1+AZ} & 0 \\ 0 & 0 & 1+\dfrac{R_0^2}{4(1+AZ)^3} \end{bmatrix} \quad (21)$$

A similar derivation of the momentum balance equation gives

$$\sqrt{1+\frac{R_0^2 A^2}{4(1+AZ)^3}}\frac{\partial T(ZS)}{\partial S} + \frac{\partial T(ZZ)}{\partial Z}$$
$$-\frac{A}{2(1+AZ)^{3/2}}(T(ZZ) - T(SS)) = 0 \quad (22)$$

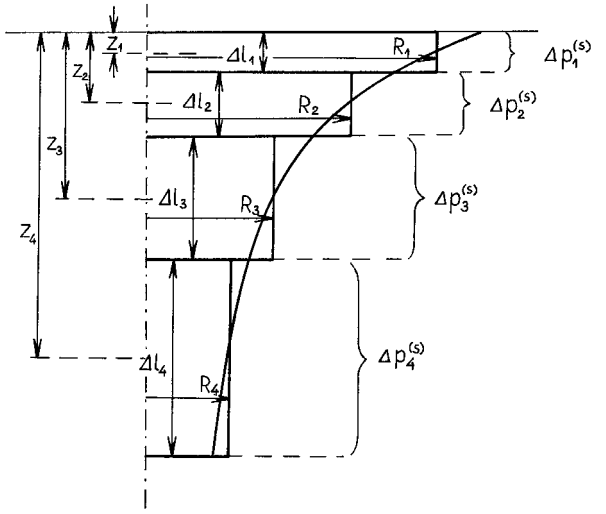

Figure 3 Diagram relating parameters in eq. (26) to the geometry of the bell-mouthed dies simplified for shear correction.

The square root factor takes into account the fact that the shear contribution is enhanced near the entrance, as the die curvature extends the effective length of the wall. For long dies, the factor tends to unity as the geometry approaches that of a parallel sided pipe. A similar situation occurs in the third term in eq. (22) corresponding to the first normal stress difference contribution due to shear. The factor in the third term tends to zero for long dies because normal stresses do not project into the axial direction for parallel sided dies.

The tangential stress gradient in the modified coordinate system can be calculated as for a long, parallel-sided channel, giving the following relationship with the axial pressure gradient:

$$\frac{\partial T(ZS)}{\partial S} = \frac{\partial p^{(s)}}{\partial Z} \cong -\frac{\Delta p_i^{(s)}}{\Delta l_i} \tag{23}$$

The shear contribution to the total pressure drop in the die is evaluated on the basis of approximation of the die curvature by a discrete set of parallel sided dies (see Figs. 3 and 4). The pressure drop for each of them can be measured experimentally, and then eq. (22) can be used to take into account the curvature of the corresponding segments of bell-mouthed die. The integration of eq. (22) along the axial direction, observing that the normal stress $T(ZZ)$ can be identified with the pressure at the inlet and the outlet and incorporating the discrete nature of the set of capillaries, gives the pressure correction, which should be subtracted from the total pressure drop in the real converging die, as follows:

$$\Delta p_{\text{corr}}^{(s)} = \sum_i \left[\sqrt{1 + \frac{R_0^2 A^2}{4(1 + AZ_i)^3}}\, \Delta p_i^{(s)} + \frac{A \Delta l_i}{2(1 + AZ_i)^{3/2}} N_{1i} \right] \tag{24}$$

where summation takes place over the set of capillaries of lengths Δl_i and axial positions of each middle point Z_i and the first normal stress difference in shear is denoted by

$$N_{1i} = (T(ZZ) - T(SS))_i \tag{25}$$

If the normal stress contribution is separated from the rest of eq. (24), then it can be simplified to

$$\Delta p_{\text{corr}}^{(s)} = \sum_i \left[\sqrt{1 + \frac{R_0^2 A^2}{4(1 + AZ_i)^3}}\, \Delta p_i^{(s)} \right] + \Delta p_{\text{norm}}^{(s)} \tag{26}$$

The last equation can be used in principle to evaluate the shear correction to the total flow in the die if the experimentally measured pressure drops in individual capillaries are substituted for $\Delta p_i^{(s)}$. A serious problem appears, however, when evaluating the normal stress contribution $\Delta p_{\text{norm}}^{(s)}$. As it is well known, the normal stress difference in shear is very sensitive to the shear rate, which in the case of a converging die is dependent on complex phenomena near the wall, including shear thinning and slippage at the wall. For example, the following relationship can be obtained for a pipe[16]:

$$\dot{\gamma}_w = \left[\frac{3n + 1}{4n} - \frac{\alpha}{4}(\beta + 3) \right] \dot{\gamma}_a \tag{27}$$

where

$$\dot{\gamma}_a = \frac{4v}{R} \quad \alpha = \frac{u_s}{v} \quad \beta = \frac{d \ln u_s}{d \ln \dot{\gamma}_a} \tag{28}$$

and v denotes the mean velocity; R, the pipe radius, and u_s, the effective slippage velocity. For high slippage, the expression in the square brackets tends to zero (as would happen in the case of a lubricated die), but, generally, it is very difficult to evaluate. Thus, the shear correction can be only obtained in practice by leaving out the $\Delta p_{\text{norm}}^{(s)}$ term. Fortunately, as will be evident from the experimental results, the normal stress contribution

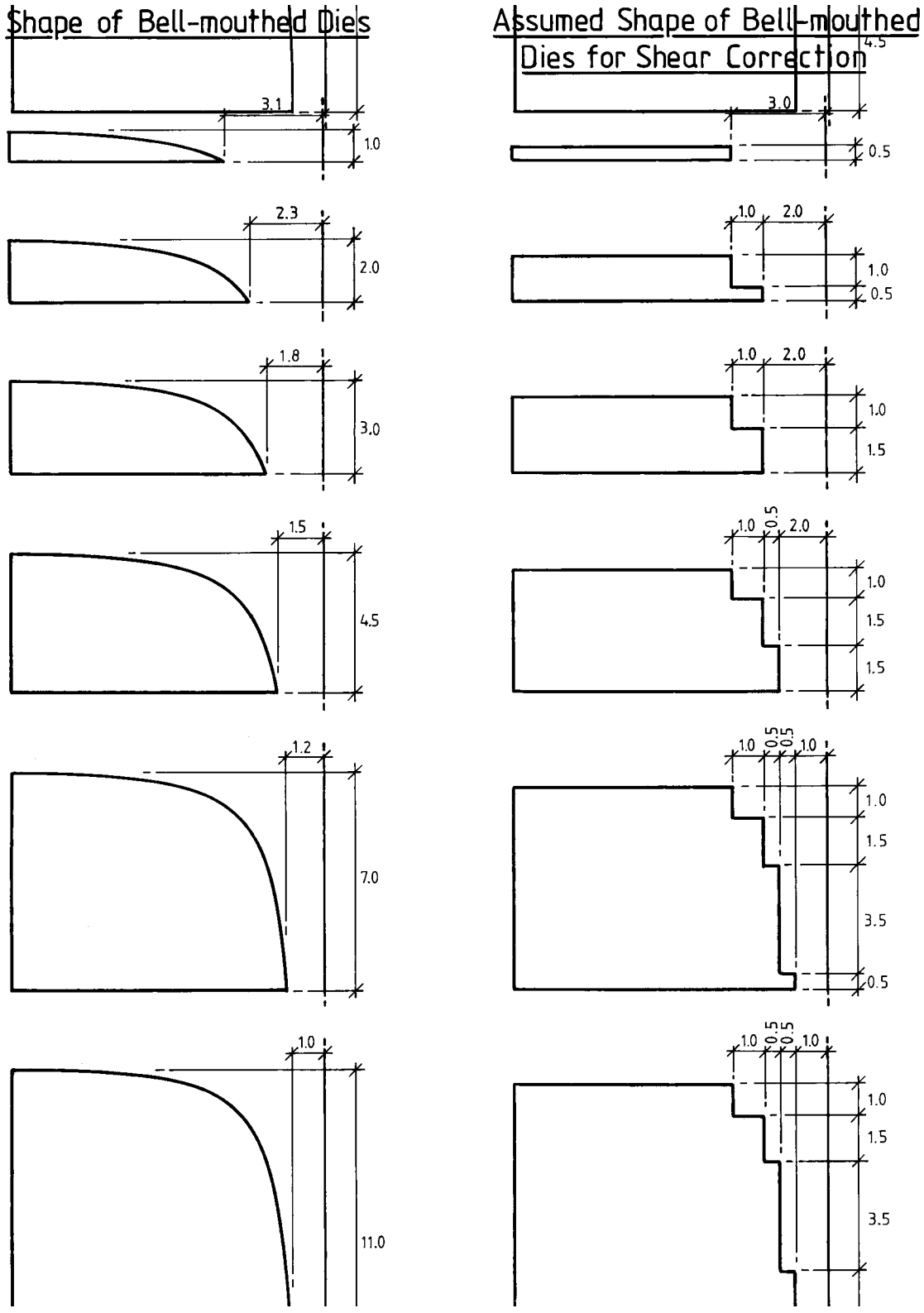

Figure 4 Geometries of bell-mouthed dies and dies simplified for shear correction.

to shear pressure drop appears to be constant with die length. Because elongational viscosity is calculated using only the slope of the straight line obtained by plotting corrected experimental pressure drops against values of $\ln(1 + AZ)$, the constant contribution of shear normal stress difference will not influence the values obtained.

EXPERIMENTAL

The study was carried out using a very simple compound containing only rubber [styrene–butadiene rubber (SBR) 1502] and 30 phr of carbon black (N330). The compound was mixed in a Francis Shaw K1 Intermix using a circulating water temperature of 30°C. The rubber was masticated for 3 min at 15 rpm before the carbon black was added, and mixing was continued at 30 rpm for 8 min further before discharge.

Elongational viscosity experiments were carried out at 90°C using a Davenport capillary rheometer fitted with bell-mouthed dies of different lengths, as shown in Figure 4. In addition, straight sided dies were used to determine the contribution of shear to pressure drop in the bell-mouthed dies. Tests were carried out with and without lubrication.

In the unlubricated tests, rubber was placed in the capillary barrel and compressed and preheated for 5 min before being extruded. A piston speed of 63 mm min^{-1} was used in all the experiments, which, according to eq. (6), corresponds to an elongational strain rate of 10 s^{-1}. Pressure drops across the dies were measured using a pressure transducer fitted flush with the barrel wall, just above the die.

In the lubricated tests, rubber samples were preformed into smooth and nonporous rods of compound using the following method. The compound was compressed and heated in the barrel of the capillary rheometer, which was sealed at the lower end. After 5 min, the plug was removed, and the rubber extruded out of the open end. The rods of compound were then spread with a layer of silicone grease (Ambersil M490) about 2 mm thick before being returned to the barrel and tested in the same way as the unlubricated compound. The preforming of the rubber was to ensure that lubrication occurred only at the interface between rubber and metal and not within the mass of rubber itself. Pressure drop values recorded for the lubricated compound tended to be rather noisy and variable, indicating that extrusion was probably occurring by a slip-stick process. The lower pressure drop values were recorded because these were most likely to correspond to full slip of the rubber at the die wall.

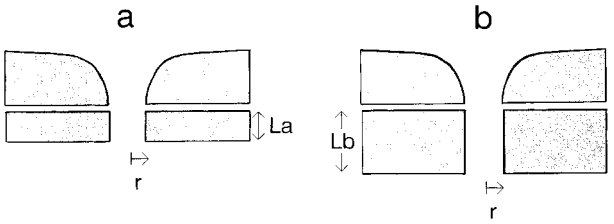

Figure 5 Diagram to show how pressure drops due to shear were determined using straight dies.

Pressure drop due to shear in the bell-mouthed dies was estimated by measuring pressure drops across parallel sided dies. For each of these measurements, a straight-sided die was placed below a bell-mouthed die, having an exit diameter as close as possible to that of the parallel-sided die, as shown in Figure 5. The reason for placing the dies in series was to ensure that the flow of rubber in the parallel sided die should be as similar as possible to the flow at an equivalent position in the bell-mouthed die. Straight-sided dies 2, 3, 4, and 6 mm in diameter were used, with two dies of different lengths for each diameter.

Values of shear stress for the compound were measured in a biconical rotor rheometer at 90°C and at strain rates between 1 and 100 s^{-1}.

RESULTS AND DISCUSSION

According to eq. (18), elongational viscosity should be equivalent to the slope of the line obtained when pressure drop due to elongation is plotted against values of $\ln(1 + AL)$ for the bell-mouthed dies. However, total pressure drops measured across the bell-mouthed dies include contributions from both elongational and shear deformation. Therefore, it was first necessary to subtract pressure drop due to shear from the total pressure drop in order to obtain pressure drop due to elongation.

Pressure drops due to shear were estimated by assuming simplified shapes for the bell-mouthed dies comprising parallel sided segments as shown in Figures 3 and 4. A theoretical estimation of the pressure drop due to shear was obtained by applying well-established equations used to de-

Table I Theoretical and Measured Values of Pressure Drop Due to Shear for the Bell-Mouthed Dies

Length of Bell-Mouthed Die (mm)	Pressure Drop Due to Shear, $\Delta p^{(s)}_{corr}$ (MPa)	
	Theoretical	Measured
1	0.3	0.3
2	0.7	0.8
3	1.2	1.3
4.5	2.3	2.4
7	4.4	4.5
11	10.0	10.1

scribe the flow of non-Newtonian fluids through capillaries. The strain rate at the wall of each die segment was determined from eq. (29), as follows:

$$\dot{\gamma}_w = \frac{3n + 1}{n} \frac{Q}{\pi R^3} \tag{29}$$

where Q is the volumetric flow rate through the die.

The corresponding shear stress (τ) was calculated using the power law relationship given in eq. (30).

$$\tau = \eta_a \dot{\gamma}^n \tag{30}$$

The non-Newtonian constant, $n = 0.2$, and apparent viscosity at 1 s^{-1}, $\eta_a = 0.181$, were obtained from an independent experiment using a rotational rheometer. The pressure drop ($\Delta p_i^{(s)}$) across each of the straight-sided segments was then calculated using eq. (31), as follows:

$$\Delta p_i^{(s)} = \frac{\tau_w 2\Delta l_i}{R_i} \tag{31}$$

Equation (26) was used to take into account the curvature of the die wall and determine the overall contribution of shear to total pressure drop for each of the bell-mouthed dies, except that the normal stress difference term ($\Delta p^{(s)}_{norm}$) was not included because it could not be quantified (Table I).

A major problem with the theoretical approach described above is that no account can be taken of slippage of the rubber against the die wall, which could lead to an overestimation of pressure drop due to shear. For this reason, it was decided to carry out direct measurements of pressure drops across individual straight-sided dies having the same diameters as the simplified die segments, as described in the experimental section. As for the theoretical calculation of pressure drop due to shear, the simplified die shapes shown in Figures 3 and 4 were assumed. Values of $\Delta p_i^{(s)}$ needed to solve eq. (26) were determined using parallel sided dies, as follows. For each pair of straight-sided dies, values of pressure drop per mm length were calculated by subtracting the pressure drop for the shorter die from that of the longer die and dividing the result by the difference in die lengths, as indicated in Figure 5. Values of $\Delta p_i^{(s)}$ were then determined by multiplying pressure drops per mm length by lengths of the corresponding straight-sided sections in the simplified dies shown in Figure 4. An example of the experimental values and dimensions used in the calculation of $\Delta p^{(s)}_{corr}$ is shown in Table II, using data from a test carried out using the 11-mm-long bell-mouthed die. Values of R_o and A used were 10 and 9.54, respectively.

Values of pressure drop due to shear determined by this experimental method are compared with those determined theoretically in Table I. If substantial slippage had occurred at the wall of the bell-mouthed die, then the experimentally measured values of pressure drop due to shear would have been lower than those determined theoretically. However, the fact that the results are so similar suggests that a negligible amount of slippage is occurring at the die wall for this compound tested under the present conditions.

Table II Experimental Values and Dimensions Used in the Calculation of Shear Contribution to Pressure Drop for the 11-mm-Long Bell-Mouthed Die (Unlubricated)

n	R_i (mm)	Pressure Drop per mm Length (MPa)	ΔI_i (mm)	Z_i (mm)	$\Delta p_i^{(s)}$ (MPa)	$\Delta p^{(s)}_{corr}$ (MPa)
1	3.0	0.3	1.0	1.0	0.30	0.5
2	2.0	0.5	1.5	1.75	0.75	1.3
3	1.5	0.7	3.5	4.25	2.45	3.8
4	1.0	1.4	4.5	8.25	6.30	10.1

Table III Pressure Drops Across Bell-Mouthed Dies Due to Elongation and Shear With and Without Lubrication

	Unlubricated			Lubricated		
Die Length (mm)	Total Pressure Drop (MPa)	Pressure Drop Due to Shear (MPa)	Pressure Drop Due to Elongation (MPa)	Total Pressure Drop (MPa)	Pressure Drop Due to Shear (MPa)	Pressure Drop Due to Elongation (MPa)
1	3.6	0.3	3.3	1.9	0	1.9
2	5.3	1.0	4.3	3.6	0	3.6
3	6.5	1.5	5.0	4.2	0	4.2
4.5	8.2	2.6	5.6	5.2	0.3	4.9
7	11.6	4.7	6.9	6.7	1.2	5.5
11	15.9	10.3	5.6	9.2	5.0	4.2

Pressure drops across bell-mouthed dies due to elongation and shear, with and without lubrication, are shown in Table III. The pressure drop due to elongation was determined by subtracting the pressure drop due to shear ($\Delta p_{\text{corr}}^{(s)}$) from the total measured pressure drop.

Figure 6 shows both total and elongational pressure drops across the bell-mouthed dies for the unlubricated system. Increasing values of $\ln(1 + AL)$ correspond to increasing die length. The total pressure drop values curve upwards with increasing die length due to the increasing contribution from shear, as would be expected with the narrowing of the die. The values of pressure drop due to elongation fall on a straight line except for the longest die, which lies below the line. The negative deviation from the line suggests that more slippage is occurring in the bell-mouthed die than in the corresponding straight die used for shear correction. The error may be due to the fact that there is an acceleration of flow through the bell-mouthed die, which could cause greater slippage than the steady rate of flow through the parallel sided die. For this die having a long, narrow section, the shear contribution to total pressure drop is considerable, and any small error in its determination will lead to a large error in the value of elongational pressure drop. For this reason, it would be advisable to use relatively short bell-mouthed dies to measure elongational viscosity and avoid those with long, narrow sections.

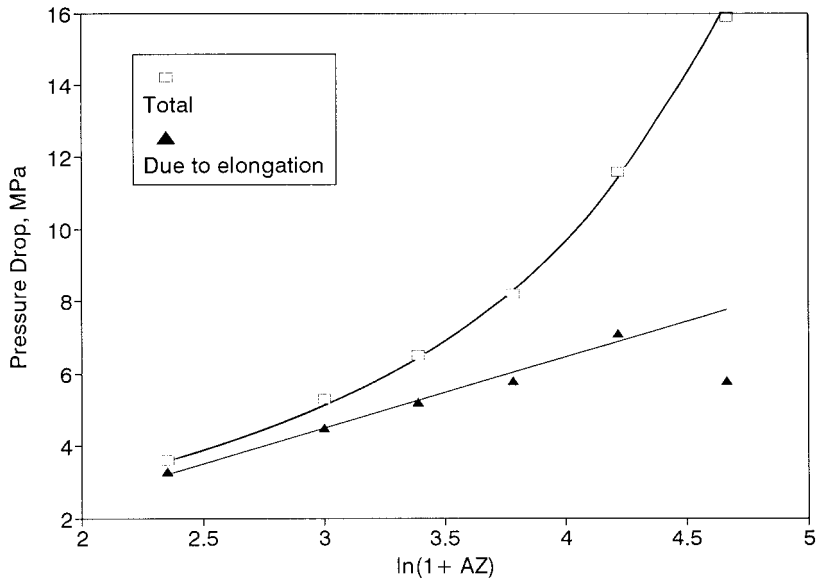

Figure 6 Total pressure drop and pressure drop due to elongation for unlubricated bell-mouthed dies.

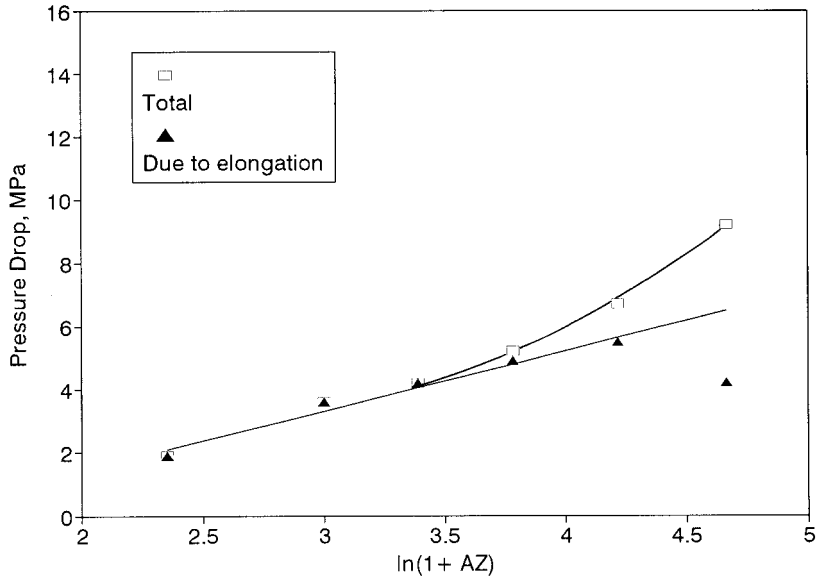

Figure 7 Total pressure drop and pressure drop due to elongation for lubricated bell-mouthed dies.

The fact that the calculated pressure drops due to elongation fall on a straight line, as predicted by eq. (18), tends to suggest that the shear correction method is generally valid. However, the pressure drop caused by the normal stress difference due to shear has not been subtracted from the total pressure drop, and so it is not possible to state with confidence that the slope of the straight line directly corresponds to elongational viscosity.

To test the validity of the experimental shear correction method, experiments were carried out with and without lubrication. Lubrication would remove or at least substantially reduce shear near the die wall and hence eliminate or minimize the shear contribution to total pressure drop, including that due to the normal stress difference. Therefore, the method of shear correction would be validated if elongational viscosity values were the same for the lubricated and unlubricated tests.

Figure 7 shows pressure drops for the lubricated system. The uncorrected data shows a much smaller upward curve of pressure drop values with increasing die length than is the case for the unlubricated system, indicating that substantial slippage occurred. Table III shows that there is no shear contribution to total pressure drop for the three shortest dies, suggesting that there is perfect slippage at the die walls. For longer dies, there is an increasing shear contribution, although this is much smaller than for the unlubricated system. The corrected data lies on a good straight line except for the longest die, as was observed for the unlubricated system.

Figure 8 shows pressure drops due to elongation for the unlubricated and lubricated systems. Lines drawn through both data sets have similar slopes of 1.9 MPa, corresponding to an elongational viscosity of 190 kPa s at 10 s^{-1}. The fact that the slopes are similar indicates that the shear correction method is a valid means of determining the elongational contribution to pressure drop and suggests that the contribution of normal stress difference due to shear is either insignificantly small or does not vary with die length. The reason for the relative displacement of the two lines along the pressure drop axis is not clear but may be due to normal stress difference in shear or may result from slippage of the rubber at the barrel wall in the lubricated tests.

CONCLUSIONS

The results indicate that for the compound used in this study, a combination of bell-mouthed and straight-sided dies can be used in a conventional capillary rheometer to determine steady-state elongational viscosity. It is very likely that the same method can be applied successfully to other rubber compounds.

Using bell-mouthed dies of the correct geometry, steady-state elongational viscosity can be calculated from a plot of pressure drop due to elongation against $\ln(1 + LA)$, where A is a geometric constant for the die and L is die length. To obtain values of pressure drop due to elongation, it is

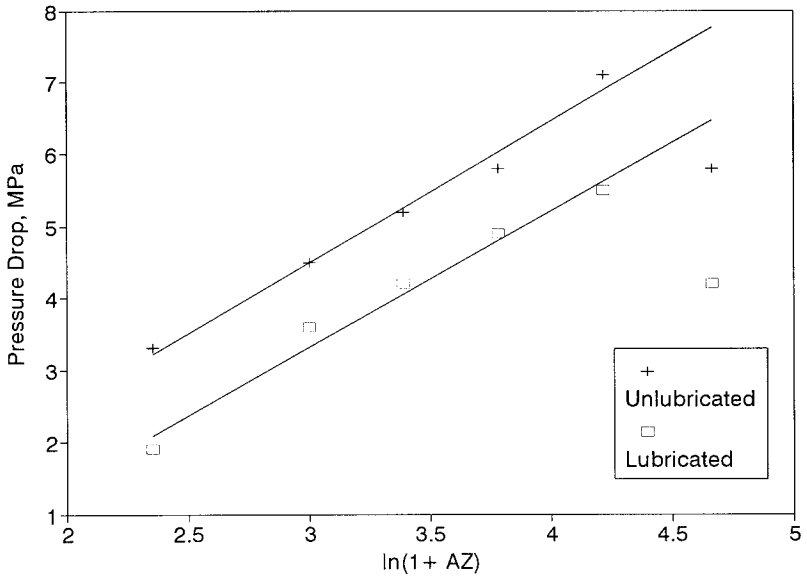

Figure 8 Pressure drop due to elongation for unlubricated and lubricated bell-mouthed dies.

necessary to correct the total pressure drop measured across the bell-mouthed dies for the contribution from shear occurring near the die wall. By assuming a simplified shape for the bell-mouthed dies and applying a formula to pressure drop data measured across straight dies, an estimate of the pressure drop due to shear is obtained. Pressure drops due to elongation are then determined by subtracting the pressure drop due to shear from the total pressure drop measured across the bell-mouthed dies. However, as the shear contribution to total pressure drop becomes very large relative to the elongational contribution, the shear correction becomes less accurate. For this reason, it would be advisable to use shorter bell-mouthed dies, avoiding those with relatively long narrow sections.

This work has been carried out with the support the Engineering and Physical Sciences Research Council and the following companies: Cabot Carbon Ltd., Francis Shaw & Co. Ltd., Pirelli Ltd., and Du Pont De Nemours (International). The authors would especially like to thank Mr. Colin Lines for skillfully making the bell-mouthed dies.

REFERENCES

1. F. N. Cogswell, *J. Non-Newtonian Fluid Mech.,* **4,** 23 (1978).
2. C. J. Petrie, *Rheol. Acta,* **34,** 12 (1995).
3. M. Funt, *Rubber Chem. Technol.,* **53,** 772 (1980).
4. G. Mason, *J. Colloid Interface Sci.,* **58,** 275 (1977).
5. N. E. Hudson, J. Ferguson, and P. Mackie, *Trans. Soc. Rheol.,* **18,** 541 (1974).
6. R. K. Gupta and T. Sridhar, in *Advances in Rheology,* Vol. 4, B. Mena, A. Garcia-Rejon, and C. Rangel-Nafaille, Eds., UNAM, 1984, p. 71.
7. D. R. Oliver and R. Bragg, *Rheol. Acta,* **13,** 830 (1974).
8. J. E. Matta and R. P. Tytus, *J. Non-Newtonian Fluid Mech.,* **17,** 215 (1990).
9. V. Tirtaatmadja and T. Sridhar, *J. Rheol.,* **37,** 1081 (1993).
10. J. Meisner, *Ann. Rev. Fluid Mech.,* **17,** 45 (1985).
11. D. M. Jones, K. Walters, and P. R. Williams, *Rheol. Acta,* **26,** 20 (1987).
12. D. F. James, G. M. Chandler, and S. J. Armour, *J. Non-Newtonian Fluid Mech.,* **35,** 421 (1990).
13. E. Everage Jr. and R. L. Ballman, *Nature,* **273,** 213 (1978).
14. J. M. Dealy, *Rheometers for Molten Plastics,* Van Nostrand Reinhold, New York, 1982.
15. D. F. James and K. Walters, in *Techniques of Rheological Measurement,* A. A. Collyer, Ed., Elsevier, New York, 1994, p. 33.
16. G. Astarita and G. Marrucci, *Principles of Non-Newtonian Fluid Mechanics,* McGraw-Hill, London, 1974.
17. R. Ariz, *Vectors, Tensors and the Basic Equations of the Basic Equations of Fluid Mechanics,* Dover Publications, New York, 1989.